H_∞ Filtering for a Giant Cavity System with Two Coupling Points

Guangpu Wu, Yuting Zhu, Tian Tang and Shibei Xue

***Abstract*— In this paper, we present an H_∞ filter for a giant cavity system which couples to a single-mode waveguide at two spatially separated points. The dynamics of the cavity is described by a time-delay Langevin equation in the Heisenberg picture whose time-delay term results from the non-local interactions to a waveguide. The input-output relation with a time-delay feature is also derived. In addition, we design an H_∞ filter for estimating the evolution of the mode in the cavity using a quadrature representation state-space representation and Linear Matrix Inequality (LMI) approach. Finally, the efficacy of our method is numerically demonstrated in an example.**

***Keywords*—Giant systems, H_∞ quantum filtering, Linear Matrix Inequality.**

I. Introduction

In recent years, the field of quantum technology has seen rapid advancements, particularly in the precise control and manipulation of increasingly complex quantum systems. A central focus in this area has been the development of coupling quantum systems [1], [2], especially those featuring structured interactions. These systems have gained significant attention due to their potential to enable new and enhanced quantum functionalities, which could revolutionize various domains, from computing to sensing. Among these, quantum systems involving giant cavities, which are essentially quantum resonators with extended spatial dimensions, coupled to waveguides, have emerged as a particularly promising platform for exploring novel quantum phenomena. These systems represent a marked difference from conventional counterparts which typically involve localized coupling. Instead, they offer a rich and intricate environment to study the interaction between spatially extended modes and propagating fields [3], [4]. However, despite their promise, the dynamics of giant cavities coupled at multiple spatial points, and the corresponding time-delay effects induced by finite propagation speeds in the waveguides, remain largely unexplored in existing literatures [5], [6].

The multi-point coupling configuration in giant cavity systems introduces distinct time-delay effects that significantly alter the system's dynamics compared to traditional quantum optical systems [7]. In most conventional systems, coupling are localized, meaning the effects of spatial separation is negligible. In contrast, the coupling in giant cavity systems is distributed across multiple spatial points, forming a time- delayed self-feedback loop. This loop depends on the spatial separation of the cavity points and the propagation characteristics of the waveguides. These time-delayed interactions result in a new way of non-Markovian effects in quantum systems. The ability to manipulate these time-delay effects provides new opportunities for developing quantum functionalities that would be inaccessible in standard cavity-QED setups [8]. The time delays in these systems can give rise to complex behaviors, such as enhanced sensitivity to external parameters, which are of critical importance for the development of applications like quantum gyroscopes and quantum memories [9], [10].

In such systems, filtering plays not only a crucial role in attenuating noise in signals, but also serves as a key tool for enhancing system performance and stability [11]–[15]. Unlike traditional quantum systems, non-local interactions result in time-delay effects leading to different dynamics of giant systems. These interactions are influenced by the spatial distribution of coupling points and the propagation characteristics of the system, resulting in delayed system responses. Form the perspective of control theory, this kind of system simultaneously exhibits state, input, and output delays, which is rarely considered in existing filtering works. In addition, existing works on filtering for quantum systems primarily focuses on Markovian systems without time delays [16]. Building upon this foundation, filtering for non-Markovian systems with colored noise has also been investigated [17]; however, in these cases, the non-Markovian effects stem from environmental memory [18]–[25]. Notably, a significant gap remains in the literature concerning the study of non-Markovian systems with inherent time delays, which is an unexplored area in the field of quantum filtering.

In order to solve the filter problem, we primarily investigate the dynamics of giant cavities with two coupling point, and focus on the inherent time-delay effects. We focus on how these time-delays affect the overall dynamics of the system, particularly the non-Markovian effects and feedback resulted. We derive the time-delay dynamical equation and the input-output equation of the system, which is given in a quadrature representation. Based on the model, we design an H_∞ filter. This filter addresses challenges in time delays that traditional filtering methods would fail to do this.

Notation For a matrix $A = [A_{s,t}]$, the symbols A^T and A^* represent the transpose and Hermitian conjugate of A. Given a complex number a, a represents its conjugate. The matrix $\mathcal{M}(A)$ is defined as $\mathcal{M}(A)_{s,t} = \frac{1}{2}\begin{bmatrix} a+a^* & i(a-a^*) \\ -i(a-a^*) & a+a^* \end{bmatrix}$. Given two operators of M and N, $[M,N] = MN - NM$ and $\{M,N\} = MN + NM$ are their commutators and anti-commutators, respectively.

*This work is supported by the National Natural Science Foundation of China (NSFC) under Grants No. 62273226 and No. 61873162.

The authors are all with Department of Automation, Shanghai Jiao Tong University, Shanghai 200240, P. R. China (Corresponding author: Shibei Xue shbxue@sjtu.edu.cn)

II. System description and modeling

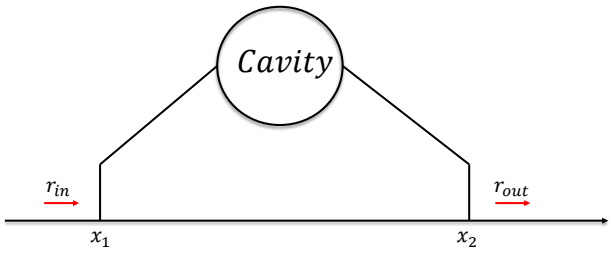

Fig. 1. Schematic of a cavity coupling to a waveguide at two points.

In this section, we consider the modeling of the giant cavity system, which consists of a cavity coupled to a single-mode waveguide at two separated coupling points, as shown in Fig. 1. The propagation of quantum fields within the waveguide plays a central role in this system. To fully describe the system, we start with its Hamiltonian, which includes contributions from the cavity, the environment and their interaction. The total Hamiltonian is given by

$$H = H_S + H_E + H_I, \tag{1}$$

where

$$H_S = \omega_c a^\dagger a, \tag{2}$$

represents the Hamiltonian of the cavity with the resonance frequency of the cavity ω_c and the creation and annihilation operators of the cavity mode $a^\dagger$ and a, respectively, with $[a, a^\dagger] = 1$. H_E describes the free Hamiltonian of the waveguide, expressed as

$$H_E = \int_{-\infty}^{+\infty} \mathrm{d}\omega\ \omega a_r^\dagger(\omega) a_r(\omega), \tag{3}$$

where $a_r^\dagger(\omega)$ and $a_r(\omega)$ are the creation and annihilation operators of the waveguide mode with frequency ω. H_I characterizes their interactions

$$H_I = \sum_{n=1}^{2} \frac{V_q}{\sqrt{v_g}} \int_{-\infty}^{\infty} \mathrm{d}\omega \big(a_r(\omega) e^{\mathrm{i}\omega\tau_n} a^\dagger + a_r^\dagger(\omega) e^{-\mathrm{i}\omega\tau_n} a \big), \tag{4}$$

where $\tau_n = x_n/v_g$ is the time delay at the coupling point $x_1 = 0$, $x_2 = L$. V_q denotes the coupling strength and v_g is the group velocity of photons in the waveguide.

In the Heisenberg picture, the time evolution of an arbitrary operator $o(t)$ is governed by the Heisenberg equation

$$\dot{o}(t) = -\mathrm{i}[o(t), H]. \tag{5}$$

The commutation of the system operator a and the cavity Hamiltonian $H_S = \omega_c a^\dagger a$ can be calculated as $[a, H_S] = \omega_c a.$ and apparently the system operator commutes with the Hamiltonian $H_E = \int_{-\infty}^{+\infty} \mathrm{d}\omega\, \omega a_r^\dagger(\omega) a_r(\omega)$; i.e., $[a, H_E] = 0$. The commutation with the interaction Hamiltonian H_I gives $[a, H_I] = \sum_{n=1}^{2} \frac{V_q}{\sqrt{v_g}} \int_{-\infty}^{\infty} \mathrm{d}\omega\, a_r(\omega) e^{i\omega\tau_n}$.

Combining these results, the equation of motion for $a(t)$ becomes

$$\dot{a}(t) = -\mathrm{i}\omega_c a(t) - \mathrm{i} \sum_{n=1}^{2} \frac{V_q}{\sqrt{v_g}} \int_{-\infty}^{\infty} \mathrm{d}\omega\, a_r(\omega) e^{\mathrm{i}\omega\tau_n}. \tag{6}$$

For the waveguide mode operators $a_r(\omega)$, the corresponding commutation can be calculated as $[a_r(\omega), H_S] = 0$, $[a_r(\omega), H_E] = \omega a_r(\omega)$, $[a_r(\omega), H_I] = \sum_{n=1}^{2} \frac{V_q}{\sqrt{v_g}} a e^{-\mathrm{i}\omega\tau_n}$, such that the equation of motion for $a_r(\omega, t)$ reads

$$\dot{a}_r(\omega, t) = -\mathrm{i}\omega a_r(\omega, t) - \mathrm{i} \sum_{n=1}^{2} \frac{V_q}{\sqrt{v_g}} e^{-\mathrm{i}\omega\tau_n} a(t), \tag{7}$$

whose solution is

$$a_r(\omega, t) = a_r(\omega, t_0) e^{-\mathrm{i}\omega(t-t_0)} - \mathrm{i} \sum_{n=1}^{2} \frac{V_q}{\sqrt{v_g}} \int_{t_0}^{t} \mathrm{d}t' a(t') e^{\mathrm{i}\omega(t'-t-\tau_n)}, \tag{8}$$

with initial time t_0. Taking Eq. (8) into Eq. (6), we have

$$\begin{aligned} \dot{a}(t) \;=\; & -\mathrm{i}\omega_c a(t) - \mathrm{i} \sum_{n=1}^{2} \frac{V_q}{\sqrt{v_g}} \int_{-\infty}^{\infty} d\omega [a_r(\omega, t_0) e^{-\mathrm{i}\omega(t-t_0)} \\ & -\mathrm{i} \sum_{n'=1}^{2} \frac{V_q}{\sqrt{v_g}} \int_{t_0}^{t} dt' a(t') e^{-\mathrm{i}\omega(t-t')} e^{-\mathrm{i}\omega\tau_{n'}}] e^{\mathrm{i}\omega\tau_n}. \end{aligned} \tag{9}$$

By using the equality $\int_{-\infty}^{+\infty} \mathrm{d}\omega e^{\mathrm{i}\omega(t-t')} = 2\pi\delta(t-t')$, we can simplify the expression further and obtain

$$\begin{aligned} \dot{a}(t) \;=\; & -\mathrm{i}\omega_c a(t) - \mathrm{i} \sum_{n=1}^{2} \frac{V_q}{\sqrt{v_g}} \int_{-\infty}^{\infty} \mathrm{d}\omega [a_r(\omega, t_0) e^{-\mathrm{i}\omega(t-t_0)} \\ & - \sum_{n=1}^{2} \sum_{n'=1}^{2} \frac{2\pi V_q^2}{v_g} \int_{t_0}^{t} \mathrm{d}t' a(t') \delta(t - t' - \tau_{n'} + \tau_n). \end{aligned} \tag{10}$$

By recalling the property of the δ function, we obtain

$$\begin{aligned} \dot{a}(t) \;=\; & -\mathrm{i}\omega_c a(t) - \mathrm{i} \sum_{n=1}^{2} \frac{V_q}{\sqrt{v_g}} \int_{-\infty}^{\infty} \mathrm{d}\omega a_r(\omega, t_0) e^{\mathrm{i}\omega(t_0 - t + \tau_n)} \\ & - \sum_{n=1}^{2} \sum_{n'=1}^{2} \frac{2\pi V_q^2}{v_g} a(t - \tau_{n'} + \tau_n) \theta(\tau_{n'} - \tau_n). \end{aligned} \tag{11}$$

Since $\tau_1 = 0$ and $\tau_2 = T$, we can derive the state-space equation incorporating the time-delay term

$$\begin{aligned} \dot{a}(t) \;=\; & -\mathrm{i}\omega_c a(t) - \mathrm{i} \sum_{n=1}^{2} \frac{V_q}{\sqrt{v_g}} \int_{-\infty}^{\infty} \mathrm{d}\omega a_r(\omega, t_0) \\ & \times e^{\mathrm{i}\omega(t_0 - t + \tau_n)} - \gamma_q \left(a(t-T) + a(t) \right). \end{aligned} \tag{12}$$

where $\gamma_q = 2\pi V_q^2/v_g$, $T = \tau_2 = x_2/v_g$. Noting that the $a_r(\omega, t)$ can be rewritten in terms of the waveguide field operator $a_{r\omega}(t)$, we now define the waveguide field $a_r(x, t)$ as

$$a_r(x, t) = \frac{1}{\sqrt{2\pi v_g}} \int \mathrm{d}\omega e^{\mathrm{i}\omega \frac{x}{v_g}} a_{r\omega}(t). \tag{13}$$

where x represents the spatial coordinate along the waveguide, and $a_r(x,t)$ captures the spatial and temporal dynamics of the field. By defining the input field as $a_r^{\text{in}} = a_r(0^-,t)$, we finally obtain

$$\begin{aligned}\dot{a}(t) &= -\mathrm{i}\omega_c a(t) - \gamma_q\big[2a(t)+a(t-T)\big] \\ &\quad -\mathrm{i}\frac{\sqrt{2\pi}V_q}{v_g}\big[a_r^{\text{in}}+a_r^{\text{in}}(t-T)\big], \end{aligned} \tag{14}$$

which captures the dynamic evolution of the cavity mode coupled to the waveguide fields.

Next, we proceed to derive the input-output relationship of the system. To begin with, we set the initial time $t_0 = 0$, which allows us to simplify the function $a_r(x,t)$. This simplification yields

$$\begin{aligned}a_r(x,t) &= \frac{1}{\sqrt{2\pi v_g}}\int \mathrm{d}\omega e^{\mathrm{i}\omega\frac{x}{v_g}}\Big[a_{r\omega}(0)e^{-\mathrm{i}\omega t} \\ &\quad -\mathrm{i}\sum_{n=1}^{2}\frac{V_q}{\sqrt{v_g}}\int_0^t \mathrm{d}t' a(t')e^{-\mathrm{i}\omega(t-t')}e^{-\mathrm{i}\omega\tau_n}\Big]. \end{aligned} \tag{15}$$

To investigate the spatial propagation of the field, we next examine the field at a position $x - v_g t$, which describes how the initial wave package propagates through the waveguide with the group velocity v_g. The expression for the field at this shifted position is

$$\begin{aligned}a_r(x-v_g t,0) &= \frac{1}{\sqrt{2\pi v_g}}\int \mathrm{d}\omega e^{\mathrm{i}\omega\frac{x-v_g t}{v_g}}a_{r\omega}(0) \\ &= \frac{1}{\sqrt{2\pi v_g}}\int \mathrm{d}\omega e^{\mathrm{i}\omega\frac{x}{v_g}}a_{r\omega}(0)e^{-\mathrm{i}\omega t}. \end{aligned} \tag{16}$$

Substituting (16) into (15), we have

$$\begin{aligned}a_r(x,t) &= a_r(x-v_g t,0) - \mathrm{i}\frac{1}{\sqrt{2\pi v_g}}\sum_{n=1}^{2}\frac{V_q}{\sqrt{v_g}}\int \mathrm{d}\omega \\ &\quad \times\int_0^t \mathrm{d}t' a(t')e^{-\mathrm{i}\omega(t-t')}e^{\mathrm{i}\omega\frac{x}{v_g}}e^{-\mathrm{i}\omega\tau_n}. \end{aligned} \tag{17}$$

Next, we perform the integration over ω to simplify the expression. This leads to

$$\begin{aligned}a_r(x,t) &= a_r(x-v_g t,0) - \mathrm{i}\frac{V_q\sqrt{2\pi}}{v_g} \\ &\quad \times\sum_{n=1}^{2} a(t-\frac{x}{v_g}+\tau_n)\theta\left(\frac{x}{v_g}-\tau_n\right). \end{aligned} \tag{18}$$

To analyze the field at specific positions, we set $x = L + 0^+$, corresponding to the waveguide output at the end of the cavity. This gives

$$\begin{aligned}a_r(L+0^+,t) &= a_r(L-v_g t,0) - \mathrm{i}\frac{V_q\sqrt{2\pi}}{v_g} \\ &\quad \times\sum_{n=1}^{2} a(t-\frac{L}{v_g}+\tau_n)\theta\left(\frac{L}{v_g}-\tau_n\right). \end{aligned} \tag{19}$$

For two coupling points, where $\tau_1 = 0$ and $\tau_2 = T = \frac{L}{v_g}$, the Eq. (19) can be further simplified as

$$\begin{aligned}a_r(L+0^+,t) &= a_r(L-v_g t,0) \\ &\quad -\mathrm{i}\frac{V_q\sqrt{2\pi}}{v_g}\big[a(t-T)+a(t)\big]. \end{aligned} \tag{20}$$

At $x = 0^-$, the field is given by $a_r(0^-,t) = a_r(-v_g t,0)$. Using the output field $a_r^{\text{out}} = a_r(L+0^+,t)$, the input-output relation becomes

$$a_r^{\text{out}}(t) = a_r^{\text{in}}(t-T) - \mathrm{i}\frac{V_q\sqrt{2\pi}}{v_g}\big[a(t-T)+a(t)\big]. \tag{21}$$

So far, we have explicitly derived the state-space equations and input-output relationships of the two-point coupled non-Markovian system through Eqs. (14) and (21), respectively.

III. H_∞ Filter Design

In this section, we develop a filter designed to estimate the system's state. The presence of delay terms in the system introduces additional complexity, making the state estimation problem more challenging. Specifically, the coupling system simultaneously exhibits state, input, and output delays, which have to be accounted for in the filter design. To model the system dynamics, we represent the coupling between the cavity and waveguide using a state-space equation that incorporates both the current and delayed states. The resulting equations are as follows

$$\begin{aligned}\dot{a}(t) &= Aa(t) + A_d a(t-T) + Bw(t) + B_d w(t-T), \\ y(t) &= Ca(t) + C_d a(t-T) + D_d w(t-T). \end{aligned} \tag{22}$$

where $A = -\mathrm{i}\omega_c - \gamma_q$ is the system matrix for the state equation. $A_d = -\gamma_q$ is the matrix governing the delayed state. $B = B_d = -\mathrm{i}\frac{\sqrt{2\pi}V_q}{v_g}$ is the input and delayed input matrices for the state equation. $C = C_d = -\mathrm{i}\frac{V_q\sqrt{2\pi}}{v_g}$ is the output matrix for the current state and the delayed state. $D_d = 1$ is the measurement matrix for the delayed input.

The output of the system is determined through homodyne detection, which is effectively modeled by the output matrices and the measurement matrix. This detection method is essential for observing the quantum state's phase and amplitude, providing a direct measurement of the field quadratures. By capturing both current and delayed states, the homodyne detection allows for a comprehensive analysis of the system's dynamics, pivotal for effective state estimation in the presence of time delays [26].

To facilitate the analysis and design of the filter, we introduce an quadrature representation state vector, $x(t)$, which includes both position and momentum components, and represents the state of the system. The real and imaginary parts of the output and input are also defined to handle the complex nature of the system. These definitions are as follows

$$x(t) = \begin{bmatrix} q(t) \\ p(t)\end{bmatrix}, \bar{w}(t) = \begin{bmatrix}\mathrm{Re}(w(t)) \\ \mathrm{Im}(w(t))\end{bmatrix}, \bar{y}(t) = \begin{bmatrix}\mathrm{Re}(y(t)) \\ \mathrm{Im}(y(t))\end{bmatrix},$$

which allow us to express the system in terms of real-valued matrices.

The quadrature representation real state-space equation, which incorporates the effects of both the current and delayed terms, is then given by

$$\begin{aligned}\dot{x}(t) &= \bar{A}x(t) + \bar{A}_d x(t-T) + \bar{B}\bar{w}(t) + \bar{B}_d\bar{w}(t-T),\\ \bar{y}(t) &= \bar{C}x(t) + \bar{C}_d x(t-T) + \bar{D}_d\bar{w}(t-T),\end{aligned} \tag{23}$$

where $\bar{A} = \mathcal{M}(A)$, $\bar{A}_d = \mathcal{M}(A_d)$, $\bar{B} = \mathcal{M}(B)$, $\bar{B}_d = \mathcal{M}(B_d)$, $\bar{C} = \mathcal{M}(C)$, $\bar{C}_d = \mathcal{M}(C_d)$, $\bar{D}_d = \mathcal{M}(D_d)$. Here, $\mathcal{M}(\cdot)$ has been defined in Section I. By expressing the system in the quadrature representation, we make it more tractable for the design of the filter, which will estimate the system's state by processing the input and output measurements while accounting for the time delay.

The time-delay filter for the time-delay system described in (23) can be designed using the following state-space equations

$$\begin{aligned}\dot{\hat{x}}(t) &= A_f\hat{x}(t) + A_F\hat{x}(t-T) + B_f\bar{y}(t),\\ \hat{y}(t) &= C_f\hat{x}(t) + C_F\hat{x}(t-T) + D_f\bar{y}(t),\end{aligned} \tag{24}$$

where $\hat{x}(t)$ is the estimated state and $\hat{y}(t)$ is the estimated output. The filter is designed to estimate the systems state from the measured output $\bar{y}(t)$, which consists of the real and imaginary parts of the measured signal. The matrices A_f, A_F, B_f, C_f, C_F, and D_f are the parameters of the filter that must be chosen to minimize the error between the actual and estimated system states.

The error state $x_e(t)$ is defined as the difference between the real system state and the estimated state, i.e., $x_e(t) = x(t) - \hat{x}(t)$. Similarly, the output error $y_e(t)$ is the difference between the real system output and the estimated output, given by $y_e(t) = y(t) - \hat{y}(t)$. The dynamics of the error state and output error can be derived as follows

$$\begin{aligned}\dot{x}_e(t) =& A_f x_e(t) + A_F x_e(t-T) + (\bar{B}_d - B_f\bar{D}_d)\bar{w}(t-T)\\ &+ \bar{B}\bar{w}(t),\end{aligned} \tag{25}$$

where $A_f = \bar{A} - B_f\bar{C}$, $A_F = \bar{A}_d - B_f\bar{C}_d$. Similarly, the equation for the output error $y_e(t)$ is derived by subtracting the filters output equation from the actual systems output equation

$$y_e(t) = C_f x_e(t) + C_F x_e(t-T) + (\bar{D}_d - D_f\bar{D}_d)\bar{w}(t-T), \tag{26}$$

where $C_f = \bar{C} - D_f\bar{C}$, $C_F = \bar{C} - D_f\bar{C}$.

Since the input noise and output noise of the system (23) are correlated white noise, traditional Kalman filtering methods become inadequate due to their fundamental assumption of uncorrelated noise. Given this correlation, it is crucial to adopt a filtering approach that can robustly handle such dependencies to ensure optimal performance under all operating conditions. The H_∞ filter addresses these challenges effectively. It is specifically designed to optimize the filter's response to worst-case scenarios, which is particularly beneficial in handling white noise. This optimization ensures the system's stability and robust performance in the face of unpredictable disturbances.

The H_∞ filtering problem can be stated as follows: Given scalars γ_1 and γ_2, find a filter with the realization of the form (24) for system (23), such that the H_∞ performance

$$\begin{aligned}J \;=\; &\langle\int_0^\infty [y_e^T(t)y_e(t) - \gamma_1^2\bar{w}^T(t-T)\bar{w}(t-T)\\ &-\gamma_2^2\bar{w}^T(t)\bar{w}(t)]\,\mathrm{d}t\rangle \le 0.\end{aligned} \tag{27}$$

is guaranteed. Based on this, we have the following main result.

Theorem 1. Given positive constants γ_1 and γ_2, if there exist positive definite matrices P, Q_1 and matrices M, D_f satisfying the matrix inequality below

$$\begin{bmatrix}\Lambda_1 & -P\bar{A}_d + M\bar{C}_d & \Lambda_2 & -P\bar{B} & \bar{C}^T D_f^T\\ \# & \Lambda_3 & 0 & 0 & \bar{C}_d^T D_f^T\\ \# & \# & -\gamma_1^2 I & 0 & \bar{D_d}^T(I - D_f)^T\\ \# & \# & \# & -\gamma_2^2 I & 0\\ \# & \# & \# & \# & -I\end{bmatrix} \le 0, \tag{28}$$

$$\begin{bmatrix}\bar{\Lambda}_1 & P\bar{A}_d - M & P\bar{B}_d - M\bar{D}_d & P\bar{B}\\ \# & 0 & 0 & 0\\ \# & \# & 0 & 0\\ \# & \# & \# & 0\end{bmatrix} \le 0, \tag{29}$$

where $\Lambda_1 = -\bar{A}^T P - \bar{C}^T M^T - P\bar{A}^T - M\bar{C} - Q_1 + \bar{C}^T\bar{C} - \bar{C}^T(D_f^T + Df)\bar{C}$, $\Lambda_2 = -P\bar{B}_d + M\bar{D}_d$, $\Lambda_3 = \bar{C}_d^T\bar{C}_d - \bar{C}_d^T(D_f^T + Df)\bar{C}_d$, $\bar{\Lambda}_1 = \bar{A}^T P + \bar{C}^T M^T + P\bar{A}^T + M\bar{C} + Q_1$, then the filter system (24) satisfies $J \le 0$, and the filter parameters are determined by

$$B_f = P^{-1}M \tag{30}$$
$$A_f = \bar{A} - B_f\bar{C}, \tag{31}$$
$$A_F = \bar{A}_d - B_f\bar{C}_d. \tag{32}$$
$$C_f = \bar{C} - D_f\bar{C}, \tag{33}$$
$$C_F = \bar{C}_d - D_f\bar{C}_d. \tag{34}$$

Proof. Firstly, we choose the Lyapunov function

$$V = \langle x_e^T(t)Px_e(t) + \int_0^t x_e^T(\tau)Q_1x_e(\tau)d\tau\rangle. \tag{35}$$

According to condition (29), we obtain $\dot{V}(t) \le 0$. Next, we rewrite the function J, including the stabilizing function $\dot{V}(t)$

$$\begin{aligned}J \;=\; &\langle\int_0^\infty [y_e^T(t)y_e(t) - \gamma_1^2\bar{w}^T(t-T)\bar{w}(t-T)\\ &-\gamma_2^2\bar{w}^T(t)\bar{w}(t) - \dot{V}(t)]\,dt + V(\infty) - V(0)\rangle\end{aligned} \tag{36}$$

It is crucial that $V(\infty) - V(0) \le 0$, ensuring that one of the

sufficient condition of $J \leq 0$ is

$$\begin{aligned} & y_e^T(t)y_e(t) - \gamma_1^2 \bar{w}^T(t-T)\bar{w}(t-T) - \gamma_2^2 \bar{w}^T(t)\bar{w}(t) \\ & +\dot{V}(t) \\ = & \begin{bmatrix} x_e(t) \\ x_e(t-T) \\ \bar{w}(t-T) \\ \bar{w}(t) \end{bmatrix}^T (\Xi_1 + \Xi_2) \begin{bmatrix} x_e(t) \\ x_e(t-T) \\ \bar{w}(t-T) \\ \bar{w}(t) \end{bmatrix} \leq 0, \end{aligned} \tag{37}$$

where Ξ_1 and Ξ_2 are matrices defined as follows

$$\Xi_1 = - \begin{bmatrix} \bar{C}^T D_f^T \\ \bar{C}_d^T D_f^T \\ \bar{D_d}^T (I - D_f)^T \\ 0 \end{bmatrix} (-I) \begin{bmatrix} D_f \bar{C} & D_f \bar{C}_d & (I - D_f)\bar{D}_d & 0 \end{bmatrix},$$

$$\Xi_2 = \begin{bmatrix} \Xi_{11} & -PA_F & -P\bar{B}_d + PB_f\bar{D}_d & -P\bar{B} \\ \# & \Lambda_3 & 0 & 0 \\ \# & \# & -\gamma_1^2 I & 0 \\ \# & \# & \# & -\gamma_2^2 I \end{bmatrix},$$

where $\Xi_{11} = -A_f^T P - PA_f - Q_1 + \bar{C}^T\bar{C} - \bar{C}^T(D_f^T + Df)\bar{C}$. Applying the Schur Complement Lemma and condition (28), we have

$$\Xi_1 + \Xi_2 = \begin{bmatrix} \Lambda_1 & -PA_F & \Lambda_2 & -P\bar{B} & \bar{C}^T D_f^T \\ \# & \Lambda_3 & 0 & 0 & \bar{C}_d^T D_f^T \\ \# & \# & -\gamma_1^2 I & 0 & \bar{D_d}^T (I - D_f)^T \\ \# & \# & \# & -\gamma_2^2 I & 0 \\ \# & \# & \# & \# & -I \end{bmatrix} \leq 0. \tag{38}$$

Thus, H_∞ performance $J \leq 0$ is satisfied. ■

IV. Simulation

In this section, we validate the proposed filter design method applied to a quantum time-delay system as defined in (23). This system comprises a single cavity coupled to a waveguide, with parameters specified as $\omega_c = 10\,\text{GHz}$, $v_g = 3000\,\text{m/s}$, and $\gamma_q = 0.1\,\text{GHz}$.

Utilizing Theorem 1, we design a filter to estimate the state of the system and mitigate estimation errors. By solving the Linear Matrix Inequality (LMI) specified in Theorem 1, we derive the following matrices

$$\begin{aligned} B_f &= \begin{bmatrix} 0.3512 & -11.6275 \\ 50.2019 & 16.8624 \end{bmatrix}, \\ A_f &= \begin{bmatrix} -5.9374 & 9.9649 \\ -8.3138 & -9.7948 \end{bmatrix}, \\ A_F &= \begin{bmatrix} -5.9374 & -0.0351 \\ 1.6862 & -9.7948 \end{bmatrix}, \\ C_f &= \begin{bmatrix} -1.1628 & 0.0649 \\ 1.5862 & -5.0202 \end{bmatrix}, \\ C_F &= \begin{bmatrix} -1.1628 & 0.0649 \\ 1.5862 & -5.0202 \end{bmatrix}. \end{aligned}$$

These matrices facilitate the computation of the filter parameters. The initial state for the real system is set to $[-1, 1]^T$.

Figs. 2 and 3 illustrate the state trajectories of the actual time-delay system and the designed filter under various delay scenarios. In these figures, the red solid line depicts the mean state trajectory of the real system, whereas the blue dotted line illustrates that of the filter. Analysis of Figs. 2 and 3 reveals that the filter effectively tracks the state of the real system across different time delays. Notably, as the time delay in the real system increases from 0.1 seconds to 0.15 seconds, there is a corresponding increase in oscillation frequency, a decrease in system stability, and an extension in the time required for the system to stabilize.

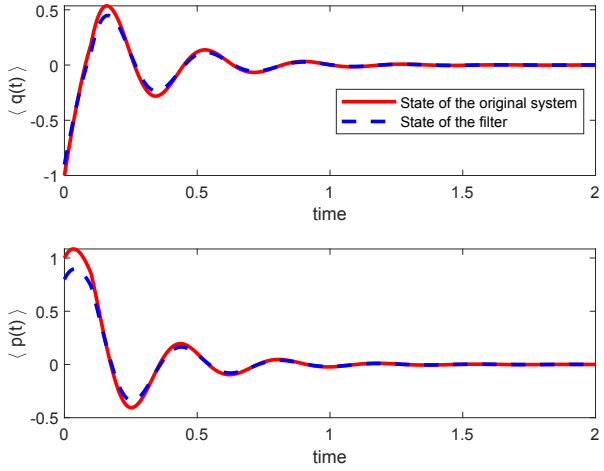

Fig. 2. The comparison of the mean values of the real system and filter states in case of delay $T = 0.1$.

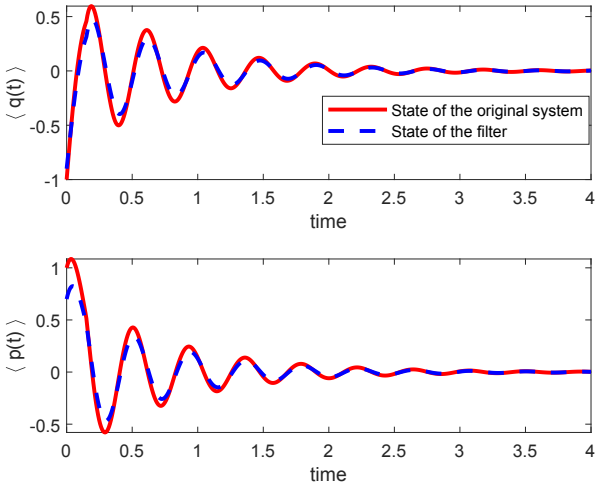

Fig. 3. The comparison of the mean values of the real system and filter states in case of delay $T = 0.15$.

V. Conclusion

This paper provides a comprehensive analysis of a quantum system characterized by a cavity coupled to a single-

mode waveguide at two spatially separated points. A significant contribution of this work lies in the development of an H_∞ filter design tailored to address the complex challenges posed by systems with simultaneous state, input, and output delays. This is accomplished through a quadrature representation state-space representation coupled with a Linear Matrix Inequality (LMI) approach. The filter design not only estimates the state of the system effectively in the presence of these delays but also ensures stability under the conditions derived theoretically. Finally, the practical applicability and performance of the proposed filter design are validated through simulation examples, demonstrating its effectiveness in managing the intricacies of delay systems. This work sets a promising foundation for future research, which includes extending to multi-coupling points systems, enhancing the efficiency of the filter under varying delay conditions, and exploring the impact of quantum noise. Additionally, the integration of real-world quantum systems into the filtering framework could offer practical insights and improvements in quantum technology applications, further expanding the scope and applicability of H-infinity filtering techniques in complex quantum systems.

REFERENCES

[1] H. Chalabi, E. Waks (2018). Interaction of photons with a coupled atom-cavity system through a bidirectional time-delayed feedback. Physical Review A, 98(6), 063832.

[2] F. Morichetti, A. Canciamilla, C. Ferrari, A. Melloni, A. Samarelli, M. Sorel, P. Velha, R. M. De La Rue, M. Martinelli (2012). The first decade of coupled resonator optical waveguides: bringing slow light to applications. Laser Photonics Reviews, 6(1), 74-96.

[3] G. Crowder, H. Carmichael, S. Hughes (2020). Quantum trajectory theory of few-photon cavity-QED systems with a time-delayed coherent feedback. Physical Review A, 101(2), 023807.

[4] L. Guo, A. F. Kockum, F. Marquardt, G. Johansson (2017). Giant acoustic atom: A single quantum system with a deterministic time delay. Physical Review A, 95(5), 053821.

[5] Y. Zhu, R. Wu, Z. Peng, S. Xue (2022). Giant-cavity-based quantum sensors with enhanced performance. Frontiers in Physics, 10, 896596.

[6] Y. Zhu, S. Xue, F. Ju, H. Yuan (2024). Quantum gyroscopes based on double-mode surface-acoustic-wave cavities. Physical Review Applied, 22(1), 014061.

[7] A. L. Grimsmo (2015). Time-delayed quantum feedback control. Physical Review Letters, 115(6), 060402.

[8] A. Carmele, B. Vogell, K. Stannigel, P. Zoller (2013). Single photon delayed feedback: a way to stabilize intrinsic quantum cavity electrodynamics. Physical Review Letters, 110(1), 013601.

[9] K. Srinivasan, O. Painter (2007). Mode coupling and cavity-quantum-dot interactions in a fiber-coupled microdisk cavity. Physical Review AAtomic, Molecular, and Optical Physics, 75(2), 023814.

[10] Y. Zhu, S. Xue, R. Wu, W. Li, Z. Peng, M. Jiang (2022). Spatial-nonlocality-induced non-Markovian electromagnetically induced transparency in a single giant atom. Physical Review A, 106(4), 043710.

[11] S. Ge, T. Vu, T. Lee (2012). Quantum measurement-based feedback control: a nonsmooth time delay control approach. SIAM Journal on Control and Optimization, 50(2), 845-863.

[12] G. Lenz, B. J. Eggleton, C. K. Madsen, R. E. Slusher (2001). Optical delay lines based on optical filters. IEEE Journal of Quantum Electronics, 37(4), 525-532.

[13] J. Wen, Y. Shi, X. Pang, J. Jia, J. Zeng (2020). Rapid stabilization of time delay stochastic quantum systems based on continuous measurement feedback. Journal of the Franklin Institute, 357(12), 7515-7536.

[14] G. Lei, Z. Yuan, Z. Yue, S. Xu, Y. Zhai (2024). Suppression of Quantum Sensor Noise using Kalman Filter for Improved Sensitivity of Single-Beam Atomic Magnetometers. Advanced Quantum Technologies, 7(4), 2300391.

[15] A. S. Mahdi, H. B. Al Husseini (2024). Filtered optical feedback modes effect on quantum-dot laser behavior. Journal of Optics, 53(3), 1972-1983.

[16] X. Meng, J. Lam, H. Gao (2008). H_∞ Filter Design for Quantum Stochastic Systems. In 2008 27th Chinese Control Conference, 525-529.

[17] S. Xue, I. R. Petersen, V. Ugrinovskii, M. R. James (2017). H_∞ Filtering For An Optical Cavity System Disturbed By Lorentzian Quantum Noise. IFAC-PapersOnLine, 50(1), 13009-13013.

[18] S. Xue, L. Y. Tan, R. B. Wu, M. Jiang, I. R. Petersen (2020). An inverse-system method for identification of damping rate functions in non-Markovian quantum systems. Physical Review A, 102(4), 042227.

[19] S. Xue, T. Nguyen, M. R. James, A. Shabani, V. Ugrinovskii, I. R. Petersen (2020). Modelling of non-Markovian quantum systems. IEEE Transactions on Control Systems Technology, 28(6), 2564-2571.

[20] S. Xue, L. Y. Tan, M. Jiang, D. W. Li (2019). A least squares identifier for a quantum non-Markovian environment model. Quantum Information Processing, 18, 310.

[21] Y. Wang, S. Xue, H. Song, M. Jiang (2023). Robust quantum teleportation via a non-Markovian channel. Physical Review A, 108(6), 062406.

[22] S. Xue, J. Zhang, I. R. Petersen (2019). Identification of non-Markovian environments for spin networks. IEEE Transactions on Control Systems Technology, 27(6), 2574-2580.

[23] S. Xue, R. B. Wu, M. R. Hush, T. J. Tarn (2017). Non-Markovian coherent feedback control of quantum dot systems. Quantum Science and Technology, 2(1), 014002.

[24] S. Xue, M. R. Hush, I. R. Petersen (2017). Feedback tracking control of non-Markovian quantum systems. IEEE Transactions on Control Systems Technology, 25(5), 1552-1563.

[25] S. Xue, R. B. Wu, W. M. Zhang, J. Zhang, C. W. Li, T. J. Tarn (2012). Decoherence suppression via non-Markovian coherent feedback control. Physical Review A, 86(5), 052304.

[26] Z. Zhao, Z. Bai, D. Jin, X. Chen, Y. Qi, J. Ding, R. P. Mildren (2022). The influence of noise floor on the measurement of laser linewidth using short-delay-length self-heterodyne/homodyne techniques. Micromachines, 13(8), 1311.